Fault-tolerant quantum repeater with atomic ensembles and linear optics

Zeng-Bing Chen,[1] Bo Zhao,[2] Yu-Ao Chen,[2] Jörg Schmiedmayer,[3] and Jian-Wei Pan[1,2]
[1]*Hefei National Laboratory for Physical Sciences at Microscale and Department of Modern Physics, University of Science and Technology of China, Hefei, Anhui 230026, China*
[2]*Physikalisches Institut, Universität Heidelberg, Philosophenweg 12, D-69120 Heidelberg, Germany*
[3]*Atominstitut der Österreichischen Universitäten, TU-Wien, A-1020 Vienna, Austria*
(Received 22 October 2006; published 23 August 2007)

We present a detailed analysis of a robust quantum repeater architecture building on the original Duan-Lukin-Cirac-Zoller (DLCZ) protocol [L.M. Duan *et al.* Nature (London) **414**, 413 (2001)]. The architecture is based on two-photon Hong-Ou-Mandel-type interference which relaxes the long-distance interferometric stability requirements by about seven orders of magnitude, from subwavelength for the single photon interference required by DLCZ to the coherence length of the photons, thereby removing the weakest point in the DLCZ scheme. Our proposal provides an exciting possibility for robust and realistic long-distance quantum communication.

DOI: 10.1103/PhysRevA.76.022329 PACS number(s): 03.67.Hk, 03.67.Pp, 42.50.−p

I. INTRODUCTION

Quantum communication ultimately aims at absolutely secure transfer of classical messages by means of quantum cryptography or faithful teleportation of unknown quantum states [1,2]. Photons are ideal quantum information carriers for quantum communication. Unfortunately, photon losses and the decrease in the quality of entanglement scale exponentially with the length of the communication channel. The quantum repeater protocol combining entanglement swapping [3,4] and purification [5] enables one to establish high-quality long-distance entanglement with resources increasing only polynomially with transmission distance [6,7].

Early physical implementations of a quantum repeater were based on atoms trapped in high-finesse cavities [8], where strong coupling between atoms and photons is required. In a seminal paper [9], Duan-Lukin-Cirac-Zoller (DLCZ) proposed an implementation of the quantum repeater by using atomic ensembles and linear optics. In this protocol atomic ensembles are used as memory qubits to avoid the challenging request for strong coupling between atoms and photons. Besides, the DLCZ protocol has built-in entanglement purification and thus is photon-loss tolerant. In the efforts of realizing the atomic ensemble based quantum repeater protocol, significant experimental advances have been achieved recently. Nonclassical correlated photon pairs were generated from a MOT and a hot vapor [10,11]. Controllable single photons were generated from atomic ensembles with the help of event-ready detection and feedforward circuit [12–14]. Entanglement between two atomic ensembles either in the same MOT or in two MOTs at a distance of 3 m were generated by detecting single photons [15,16]. Recently, a segment of the DLCZ protocol was demonstrated [17].

However, the DLCZ protocol has an inherent drawback which is severe enough to make long-distance quantum communication extremely difficult. Entanglement generation and entanglement swapping in the DLCZ protocol depend on a single-photon Mach-Zehnder-type interference. The relative phase between two remote entangled pairs is sensitive to path length instabilities, which has to be kept constant within a fraction of the photon's wavelength. Moreover, entanglement generation and entanglement swapping are probabilistic. If connecting neighboring entangled pairs does not succeed after performing entanglement swapping, one has to repeat all previous procedures to reconstruct the entangled pairs. This means that the phase fluctuations must be stabilized until the desired remote entangled pairs are successfully generated. A particular analysis shows that (see details below), to maintain path length phase instabilities at the level of $\lambda/10$ (λ is the wavelength; typically $\lambda \sim 1$ μm for photons generated from atomic ensembles) requires the fine control of timing jitter at a subfemtosecond level over a time scale of a few tens of seconds. This is almost an experimentally forbidden technique as compared with the lowest reported jitter in fiber even for kilometer-scale distances [18].

In a recent paper [19], we proposed a robust quantum repeater architecture building on the DLCZ protocol. The architecture is based on the two-photon Hong-Ou-Mandel-type interference [20–23], which is insensitive to phase instability. The path length fluctuations should be kept on the length scale within a fraction of the photons coherence length (say, 1/10 of the coherence length, which is about 3 m for photons generated from atomic ensembles [12]). Therefore the robustness is improved about seven orders of magnitude higher in comparison with the single-photon Mach-Zehnder-type interference in the DLCZ protocol.

In this paper, we give a particular analysis on the phase stability problem in the DLCZ protocol and discuss the robust quantum repeater architecture in detail. The paper is organized as follows. In Sec. II we review the original DLCZ protocol and show why the phase stability problem in the DLCZ protocol is so severe that it makes a long-distance quantum communication extremely difficult. Section III presents a detailed analysis of the robust quantum repeater based on the two-photon Hong-Ou-Mandel-type interference. A comparison with other atomic ensemble based quantum repeater protocols is also discussed. Finally, we shall summarize and draw some conclusions.

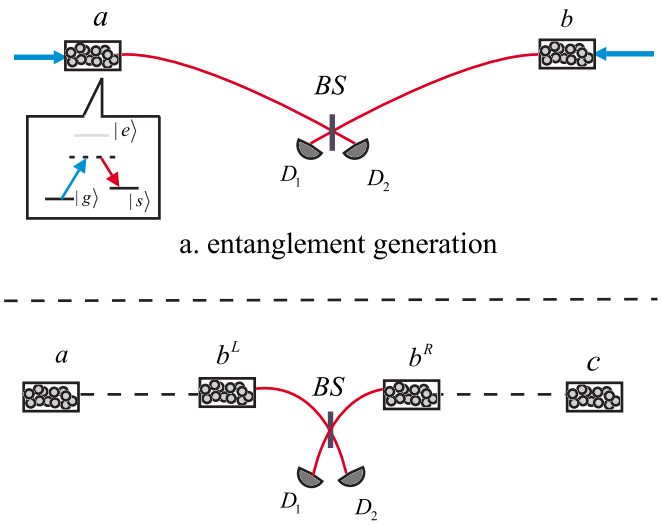

FIG. 1. (Color online) Setups for entanglement generation and entanglement swapping in the DLCZ protocol. (a) Forward-scattered Stokes photons, generated by an off-resonant write laser pulse via spontaneous Raman transition, are directed to the beam splitter (BS) at the middle point. Entanglement is generated between atomic ensembles at sites a and b, once there is a click on either of the detectors. The inset shows the atomic level structure, with the ground state $|g\rangle$, metastable state $|s\rangle$, and excited state $|e\rangle$. (b) Entanglement has been generated between atomic ensembles (a,b^L) and (b^R,c). The atomic ensembles at site b are illuminated by near resonant read laser pulses, and the retrieved anti-Stokes photons are subject to BS at the middle point. A click on either of the detectors will prepare the atomic ensembles at a and c into an entangled state.

II. DLCZ PROTOCOL

A. Review of DLCZ protocol

Let us first consider a pencil-shaped atomic sample of N atoms with Λ level structure (see inset in Fig. 1). The write laser pulse induces a spontaneous Raman process, which prepares the forward-scattered Stokes mode and collective atomic state into a two mode squeezed state [9]. The light-atom system can be described as

$$|\psi\rangle = |0_a 0_s\rangle + \sqrt{\chi} S^\dagger a^\dagger |0_a 0_s\rangle \tag{1}$$

by neglecting higher-order terms, where $|0_a\rangle = \otimes_i |g\rangle_i$ is the ground state of the atomic ensemble and $|0_s\rangle$ denotes the vacuum state of the Stokes photons. Here, $a^\dagger$ is the creation operator of the Stokes mode, and the collective atomic excitation operator is defined by $S^\dagger = \frac{1}{\sqrt{N}} \Sigma_i |s\rangle_i \langle g|$, where $|s\rangle$ is the metastable atomic state. The small excitation probability $\chi \ll 1$ can be achieved by manipulating the write laser pulse [24].

The entanglement generation setup is shown in Fig. 1(a). Let us consider two atomic ensembles at sites a and b at a distance of $L_0 \leqslant L_{att}$, with L_{att} the channel attenuation length. The Stokes photons generated from both sites are directed to the beam splitter (BS) at the middle point. Once there is a click on the detectors, entanglement between communication sites a and b is established.

The entanglement swapping setup is depicted in Fig. 1(b). Assume we have created entangled states between atomic ensembles (a,b^L) and (b^R,c), where b^L and b^R are at the same site. The two atomic ensembles at site b are illuminated simultaneously by read laser pulses. The retrieved anti-Stokes photons are subject to the BS, and a click on either of the single photon detectors will prepare the atomic ensembles at sites a and c into an entangled state. The entangled pair can be connected to arbitrary distance via entanglement swapping.

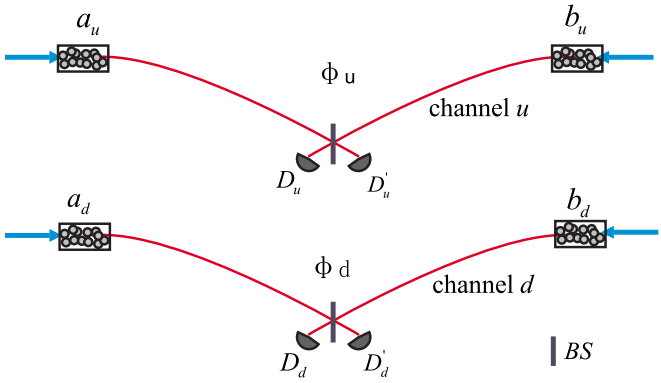

FIG. 2. (Color online) In the DLCZ protocol, two entangled pairs are generated in parallel. The relative phase between the two entangled states has to be stabilized during the entanglement generation process.

B. Phase instability analysis I

In the DLCZ protocol, the single-photon Mach-Zehnder interference is used in both entanglement generation and entanglement swapping process. Thus the phase is sensitive to path length fluctuations on the order of photons' subwavelength. Note that to implement quantum cryptography or Bell inequality detection, one has to create two pairs of entangled atomic ensembles in parallel [9]. The entanglement generated between the two pairs of atomic ensembles is equivalent to a polarization maximally entangled state. In this case, the relative phase between the two entangled pairs needs to be stabilized, which is helpful to improve the phase instability [17]. However, the requirement to stabilize the relative phase in the DLCZ scheme is still extremely demanding for current techniques.

As shown in Fig. 2, in the entanglement generation process the entanglement is established between the atomic ensembles (a_u,b_u) and (a_d,b_d) in parallel during a time interval $t_0 = T_{cc}/\chi e^{L_0/L_{att}}$, where $T_{cc} = L_0/c$ is the classical communication time. Note that one requests $2^n \chi \ll 1$ to make the overall fidelity imperfection small, where n is the connection level [9]. The entanglement generated between the two pairs of atomic ensembles can be described by

$$|\psi_{\phi_u}\rangle_{a_u,b_u} = (S^\dagger_{a_u} + e^{i\phi_u} S^\dagger_{b_u})/\sqrt{2}|\text{vac}\rangle, \tag{2}$$

$$|\psi_{\phi_d}\rangle_{a_d,b_d} = (S^{\dagger}_{a_d} + e^{i\phi_d} S^{\dagger}_{b_d})/\sqrt{2}|\text{vac}\rangle, \quad (3)$$

where $\phi_u = kx_u$ ($\phi_d = kx_d$) denotes the difference of the phase shifts in the left and the right sides of channel u (d), with x_u (x_d) the length difference between the left and the right side channel u (d). Here k is the wave vector of the photons. For simplicity we have assumed the lasers on the two communication nodes have been synchronized, and the phase instability is caused by the path length fluctuations. The entanglement generated in this process is equivalent to a maximally entangled polarization state between the four atomic ensembles,

$$|\psi_{\delta\phi}\rangle_{PME} = (S^{\dagger}_{a_u} S^{\dagger}_{b_u} + e^{i\delta\phi} S^{\dagger}_{a_d} S^{\dagger}_{b_d})/\sqrt{2}|\text{vac}\rangle, \quad (4)$$

where the relative phase between the entangled states of the two pairs of the remote ensembles is denoted by $\delta\phi = k\delta x$ with $\delta x = x_u - x_d$.

In practice, a series of write pulses are sent into the atomic ensembles and the induced Stokes pulses are directed to the detectors. The time interval between neighboring write pulses is larger than the classical communication time. When there is a click on the detectors, the entanglement is generated and classical information is sent back to the communication nodes to stop the subsequent write pulses. In this case, the change of environment due to imperfections will always induce path length fluctuations and thus phase instability. If the entanglement between the two pairs of memory qubits is always established at the same time, one can consider the Stokes photons detected at the same time experience in the same environment. Thus it is easy to find $\delta x = x_u - x_d = 0$ and no phase stabilization is needed.

However, the entanglement generation process is probabilistic. The experiment has to be repeated about $1/(\chi e^{-L_0/L_{att}})$ times to ensure that there is a click on the detectors. The two phases ϕ_u and ϕ_d achieved at different runs of the experiments are usually different due to the path length fluctuations in this time interval. For instance, the entanglement between the first pair may be constructed after the first run of the experiment, and thus we get the phase $\phi_u = kx_u$, while the entanglement between the second pair may be established until the last run of the experiment, and thus we obtain the phase $\phi_d = kx_d$. Therefore to get a high fidelity entangled pair, the relative phase $\delta\phi = k\delta x$ has to be stabilized during the whole length of the communication. To stabilize the phase instability within $\delta\phi \leqslant 2\pi/10$, one must control the path length instability $\delta x \leqslant 0.1$ μm during the whole entanglement generation process.

The path length instability is equivalent to the timing jitter of the arrival time of the Stoke pulses after transmitting the channel over kilometer-scale distances. To stabilize the path length instability $\delta x = c\delta t \leqslant 0.1$ μm, the timing jitter δt of the Stokes pulse must be controlled on the order of subfemtosecond.

The time needed in the entanglement generation process can be estimated as follows. The distance between two communication sites is considered to be $L_0 = 10$ km, and thus the classical communication time $T_{cc} = L_0/c$ is about 33 μs. Usually we have $2^n \approx 100$, and thus $\chi \approx 0.0001$. In optical fibers, the photon loss rate is considered to be 2 dB/km for photons at a wavelength of about 800 nm, and thus the duration t_0 of the entanglement generation process can be estimated to be about 30 s. Therefore phase stabilization in DLCZ protocol requires that over a time scale of about a few tens of seconds, one must control the timing jitter after transferring a pulse sequence over several kilometers on the order of subfemtosecond. This demand is extremely difficult for current technology. The lowest reported jitter for transferring of a timing signal over kilometer-scale distances is a few tens of femtoseconds for averaging times of $\geqslant 1$ s [18], which is two orders of magnitude worse than the timing jitter needed in the DLCZ protocol. In free space, the photon loss rate is about 0.1 dB/km and t_0 is about 0.5 s. In this case, the path length instability due to atmosphere fluctuations is even worse. The timing jitter is on the order of a few nanoseconds over a time scale of 1 s.

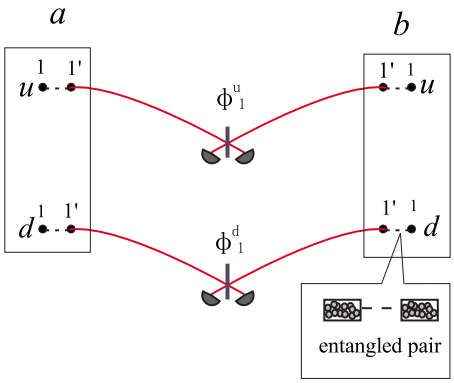

FIG. 3. (Color online) Elementary entangled pairs are created locally. Entanglement swapping is performed remotely to connect atomic ensembles between adjacent nodes a and b.

C. Phase instability analysis II

From the above analysis, we know that in the standard DCLZ protocol, the requirement to stabilize the relative phase between the two entangled pairs is severe even in the entanglement generation stage. One may consider if entanglement generation is performed locally, the time needed in the entanglement generation process is short and thus the requirement can be alleviated. However, that is not the case. It is a misunderstanding that the phase only needs to be stabilized in the entanglement generation process. In the DLCZ protocol, the single-photon Mach-Zehnder interference is also utilized in the entanglement swapping process. When performing entanglement swapping to connect the neighboring communication nodes, the phases have to be stabilized too. In the following, we will give a detailed analysis to show that the phases between neighboring nodes have to be stabilized until the desired remote entangled pairs are constructed.

Suppose elementary entangled pairs are created locally at each node and the entanglement between neighboring nodes is generated via entanglement swapping, as shown in Fig. 3. In the entanglement swapping process, one has to send pulse sequences over a long distance and thus the path length fluc-

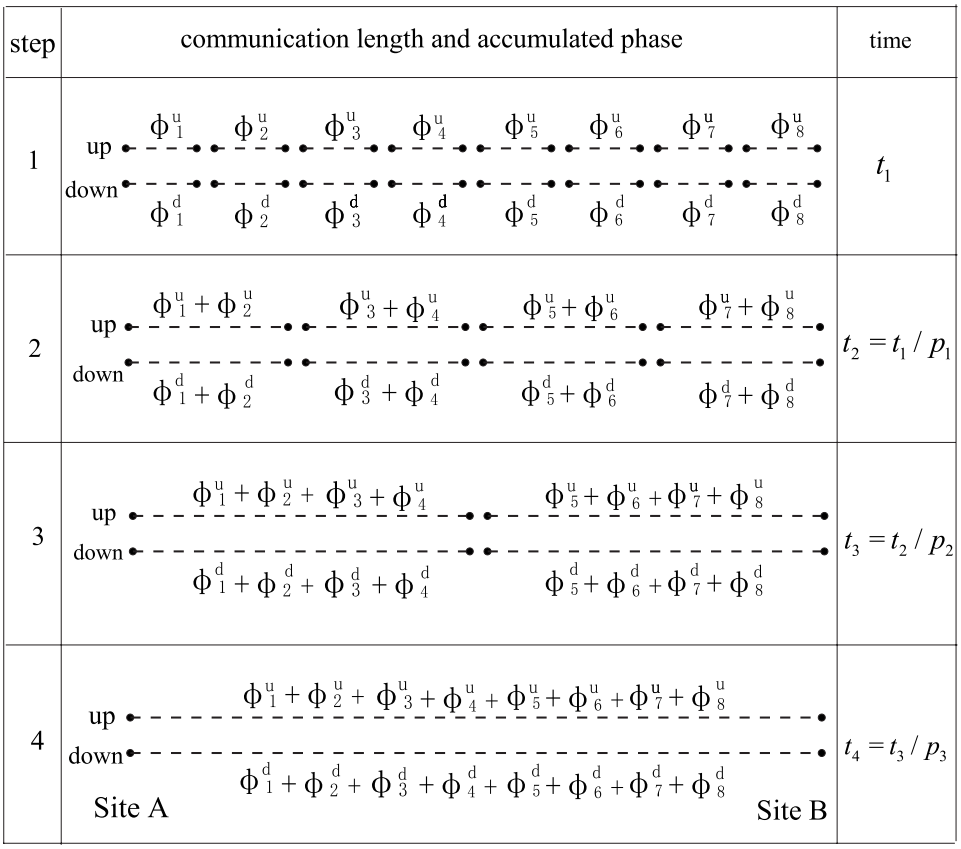

FIG. 4. Entangled pairs are generated between neighboring communication nodes as shown in Fig. 3. The entangled pairs are connected by performing further entanglement swapping to construct entanglement between remote communication sites A and B. The entanglement connection process, as well as the accumulated phase, is shown step by step.

tuations have to be controlled. The two entangled pairs obtained after entanglement swapping can be described by

$$|\psi_{\phi_1^u}\rangle_{a_{u_1},b_{u_1}} = (S^\dagger_{a_{u_1}} + e^{i\phi_1^u} S^\dagger_{b_{u_1}})/\sqrt{2}|\text{vac}\rangle, \tag{5}$$

$$|\psi_{\phi_1^d}\rangle_{a_{d_1},b_{d_1}} = (S^\dagger_{a_{d_1}} + e^{i\phi_1^d} S^\dagger_{b_{d_1}})/\sqrt{2}|\text{vac}\rangle. \tag{6}$$

Assume we are going to create the *up* and *down* entangled pairs between two remote communication sites A and B at a distance of $L=2^3L_0$. The entanglement connection process is shown step by step in Fig. 4. The entangled pairs between neighboring nodes are created as shown in Fig. 3 and then connected via further entanglement swapping which is also performed locally. After four steps, two remote entangled pairs between sites A and B are created,

$$|\Psi_{\Phi_u}\rangle_{A_u,B_u} = (S^\dagger_{A_u} + e^{i\Phi_u} S^\dagger_{B_u})/\sqrt{2}|\text{vac}\rangle, \tag{7}$$

$$|\Psi_{\Phi_d}\rangle_{A_d,B_d} = (S^\dagger_{A_d} + e^{i\Phi_d} S^\dagger_{B_d})/\sqrt{2}|\text{vac}\rangle, \tag{8}$$

where the accumulated phases are $\Phi_u=\Sigma_i\phi_i^u$ and $\Phi_d=\Sigma_i\phi_i^d$. The effectively maximally entangled pair can be described as

$$|\Psi_{\delta\Phi}\rangle_{PME} = (S^\dagger_{A_u} S^\dagger_{B_u} + e^{i\delta\Phi} S^\dagger_{A_d} S^\dagger_{B_d})/\sqrt{2}|\text{vac}\rangle, \tag{9}$$

where $\delta\Phi=\Phi_u-\Phi_d=\Sigma_i(\phi_i^u-\phi_i^d)$ is the phase difference between the *up* and *down* entangled pairs. Note that the phases ϕ_i^u or ϕ_i^d $(i=1,2,\ldots,8)$ between different nodes are independent from each other, and thus phase stabilization requires $\phi_i^u=\phi_i^d$ $(i=1,2,\ldots,8)$.

Because entanglement swapping in every step is probabilistic, if the entanglement swapping does not succeed in one step, one has to repeat all the previous steps to reconstruct the entangled pairs. In this case, the phase has to be stabilized until the desired entangled pairs $|\Psi_{\Phi_u}\rangle_{A_u,B_u}$ and $|\Psi_{\Phi_d}\rangle_{A_d,B_d}$ are both generated. For example, suppose after step 3 we have created two *up* entangled pairs and two *down* entangled pairs in parallel. In step 4, we will connect the *up* and *down* pairs, respectively, via entanglement swapping to obtain the two desired entangled pairs between remote sites A and B. Since entanglement swapping is probabilistic, it could be that we succeed in connecting the *up* pairs and acquiring $|\Psi_{\Phi_u}\rangle_{A_u,B_u}$, but fail to connect the *down* pairs after performing entanglement swapping once. In this case, we have to repeat steps 1, 2, and, 3 to reconstruct the two *down* entangled pairs and then connect them by entanglement swapping to obtain $|\Psi_{\Phi_d}\rangle_{A_d,B_d}$. Since the phase Φ_u of the *up* pair has been fixed, the phases of the *down* pairs ϕ_i^d $(i=1,2,\ldots,8)$ have to be stabilized to satisfy $\phi_i^u=\phi_i^d$ $(i=1,2,\ldots,8)$, until the *down* pair $|\Psi_{\Phi_d}\rangle_{A_d,B_d}$ is successfully generated. The total time needed in these processes is $t_4=t_1/(p_1p_2p_3)$. In other words, the phases ϕ_i^u $(i=1,2,\ldots,8)$ and ϕ_i^d $(i=1,2,\ldots,8)$ have to be stabilized over a time interval $t_4=t_1/(p_1p_2p_3)$, until the desired remote entangled pairs $|\Psi_{\Phi_u}\rangle_{A_u,B_u}$ and $|\Psi_{\Phi_d}\rangle_{A_d,B_d}$ are both generated. For long-distance quantum communication, the total time needed is on the order of several hours [25]. Even in the ideal case, it is still on the order of a few seconds. Therefore phase stabilization in the DLCZ protocol requires that one has to stabilize the path length fluctuations over a long time interval after

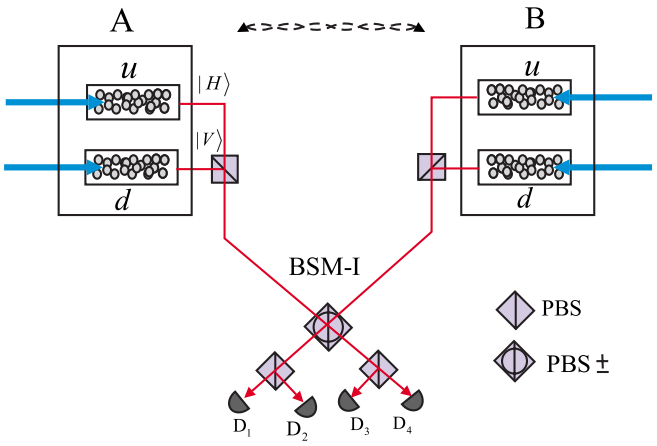

FIG. 5. (Color online) Setup for entanglement generation between sites A and B. Forward-scattered Stokes photons, generated by an off-resonant write laser pulse via spontaneous Raman transition, are subject to BSM-i at the middle point. The Stokes photons generated at the same site are assumed to have different polarization, i.e., $|H\rangle$ and $|V\rangle$. PBS (PBS$_{\pm}$) reflects photons with polarization $|V\rangle$ ($|-\rangle$) and transmits photons with polarization $|H\rangle$ ($|+\rangle$), where $|\pm\rangle=\frac{1}{\sqrt{2}}(|H\rangle\pm|V\rangle)$. After passing through the PBS$_{\pm}$ and PBS successively, the Stokes photons are detected by single photon detectors. A coincidence count between single photon detectors D_1 and D_4 (D_1 and D_3) or D_2 and D_3 (D_2 and D_4) will project the four atomic ensembles into the complex entangled state $|\psi\rangle_{AB}$ up to a local unitary transformation.

sending a pulse sequence over kilometer-scale distances. As we discussed above, it is extremely difficult for the current technique to meet this demanding requirement.

III. ROBUST QUANTUM REPEATER

A. Basic protocol

The phase stability problem could be overcome by interfering two photons [26–28]. Based on this, we proposed a robust quantum repeater architecture by taking advantage of two-photon Hong-Ou-Mandel interference [19]. In this section, we will give a detailed analysis of the protocol.

To exploit the advantage of two-photon interference, it is natural to extend the DLCZ protocol by polarization encoding a memory qubit with two atomic ensembles [16,29] and entangling two memory qubits at neighboring sites via a two-photon Bell-state measurement (BSM). Unfortunately, as shown below, the BSM will not create the desired entangled state, but a complex superposition state with spurious contributions from second-order excitations, which preclude further entanglement manipulation.

Let us consider two communication sites A and B at a distance of L_0. A schematic setup of entanglement generation is shown in Fig. 5. Each site has two atomic ensembles encoded as one memory qubit and the two atomic ensembles at each node are excited simultaneously by write laser pulses. We assume the Stokes photons generated from the two atomic ensembles at the same site have an orthogonal polarization state, e.g., $|H\rangle$ and $|V\rangle$, which denote horizontal and vertical linear polarization, respectively. In this way the memory qubit is effectively entangled in the polarization states of the emitted Stokes photons.

The Stokes photons generated from both sites are directed to the polarization beam splitter (PBS) and subject to BSM-I at the middle point to entangle the two neighboring memory qubits. However, the two-photon state generated in the second-order spontaneous Raman process will also induce coincidence counts on the detectors. Thus the BSM-I can only prepare the neighboring memory qubits into a complex superposition state with spurious contributions from second-order excitations. For instance, a coincidence count between D_1 and D_4 projects the two memory qubits into

$$|\psi\rangle_{AB}=\left[\frac{e^{i(\phi_A+\phi_B)}}{2}(S_{u_A}^{\dagger}S_{u_B}^{\dagger}+S_{d_A}^{\dagger}S_{d_B}^{\dagger})+\frac{1}{4}(e^{i2\phi_A}S_{u_A}^{\dagger 2}+e^{i2\phi_B}S_{u_B}^{\dagger 2}-e^{i2\phi_A}S_{d_A}^{\dagger 2}-e^{i2\phi_B}S_{d_B}^{\dagger 2})\right]|\mathrm{vac}\rangle, \quad (10)$$

where ϕ_A and ϕ_B are the phases that the photons acquire, respectively, from sites A and B during the BSM-I. The atomic ensembles are distinguished by subscript (u,d) and (A,B). The first part is the maximally entangled state needed for further operations, while the second part is the spurious two-excitation state coming from second-order excitations. The success probability is on the order of $O(\chi^2\eta_1^2e^{-L_0/L_{att}})$, where η_1 is the detection efficiency. The time needed in this process is $T_0\approx\frac{T_{cc}}{\chi^2\eta_1^2e^{-L_0/L_{att}}}$.

It is obvious that the phases ϕ_A and ϕ_B only lead to a multiplicative factor $e^{i(\phi_A+\phi_B)}$ before the desired entangled state and thus have no effect on the desired entanglement. The price to pay is that some spurious coincidence counts from the two-excitation terms are also registered, which obviously prevents further entanglement manipulation and must be eliminated by some means. However, we find that it is not necessary to worry about these terms because they can be automatically washed out if the BSM in the entanglement swapping step is carefully designed. In the ideal case a maximally entangled state can be created by implementing entanglement swapping.

The entanglement swapping setup is depicted in Fig. 6. Let us consider three communication sites A, B, and C, and assume that we have created the complex entangled states (Eq. (10)) $|\psi\rangle_{AB_L}$ and $|\psi\rangle_{B_RC}$ between (A,B_L) and (B_R,C), respectively [30]. The memory qubits B_L and B_R at site B are illuminated simultaneously by read laser pulses. The retrieved anti-Stokes photons are subject to BSM-II. Note that the sequence of the PBSs in BSM-II is different from BSM-I. The BSM-II is designed like this in order that the two-photon states converted from the spurious two-excitation terms are directed into the same output and thus will not induce a coincidence count on the detectors. In the ideal case, if the retrieve efficiency is unity and perfect photon detectors are used to distinguish photon numbers, only the two-photon coincidence count will be registered and project the memory qubits into a maximally entangled state. For instance, when a coincidence count between D_1 and D_4 is registered one will obtain

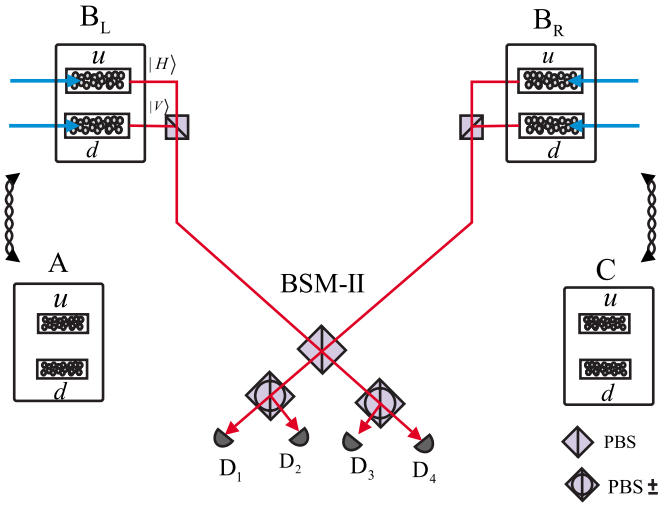

FIG. 6. (Color online) Setup for entanglement connection between sites A and C via entanglement swapping. Complex entangled states have been prepared in the memory qubits between sites (A,B_L) and (B_R,C). The memory qubits at site B are illuminated by near resonant read laser pulses, and the retrieved anti-Stokes photons are subject to BSM-ii at the middle point. The anti-Stokes photons at the same site have different polarizations $|H\rangle$ and $|V\rangle$. After passing through PBS and PBS$_{\pm}$ successively, the anti-Stokes photons are detected by single photon detectors. Coincidence counts between D_1 and D_4 (D_1 and D_3) or D_2 and D_3 (D_2 and D_4) are registered. The memory qubits will be projected into an effectively maximally entangled state ρ_{AC} up to a local unitary transformation. Note that the sequence of PBSs in BSM-II is different from BSM-I. This helps to eliminate the spurious contributions from second-order excitations.

$$|\phi^+\rangle_{AC} = (S^\dagger_{u_A} S^\dagger_{u_C} + S^\dagger_{d_A} S^\dagger_{d_C})/\sqrt{2}|\text{vac}\rangle. \tag{11}$$

In this way a maximally entangled state across sites A and C is generated by performing entanglement swapping. The maximally entangled state can be extended by further entanglement swapping as usual. Both the entanglement creation and entanglement connection in our scheme rely on two-photon interference, so the improvement in insensitivity to path length fluctuations, as compared to the DLCZ scheme, is about seven orders of magnitude.

In practice, the retrieve efficiency η_r is determined by the optical depth of the atomic ensembles [31], and current single photon detectors are incapable of distinguishing photon numbers. Taking into account these imperfections, the multiphoton coincidence counts in the BSM-II have to be considered. Through some simple calculations, one can find that the coincidence counts will prepare the memory qubits into a mixed entangled state of the form

$$\rho_{AC} = p_2\rho_2 + p_1\rho_1 + p_0\rho_0, \tag{12}$$

where the coefficients p_2, p_1, and p_0 are determined by the retrieve efficiency and detection efficiency (see the Appendix, Sec. 1 for details). Here $\rho_2 = |\phi^+\rangle_{AC}\langle\phi^+|$ is a maximally entangled state, ρ_1 is a maximally mixed state, where only one of the four atomic ensembles has one excitation, and ρ_0 is the vacuum state that all the atomic ensembles are in the ground states.

It is easy to see that ρ_{AC} is in fact an effectively maximally entangled state, which can be projected automatically to a maximally entangled state in the entanglement-based quantum cryptography schemes. When implementing quantum cryptography via the Ekert protocol [2], we randomly choose the detection basis at the remote sites and detect the photons retrieved from the atomic ensembles. Then we compare the detection basis by classical communication. In this process, only the coincidence counts are registered and used for quantum cryptography. In our case only the first term ρ_2 will contribute to a coincidence count between the detectors at the two sites and will be registered after classical communication. The maximally mixed state term ρ_1 and the vacuum term ρ_0 have no contribution to the experimental results, and thus ρ_{AC} is equivalent to the Bell state $|\phi^+\rangle_{AC} = (S^\dagger_{u_A} S^\dagger_{u_C} + S^\dagger_{d_A} S^\dagger_{d_C})/\sqrt{2}|\text{vac}\rangle$.

B. Entanglement connection and scalability

The effectively entangled state can be connected to longer communication distance via further entanglement swapping. To implement a quantum repeater protocol, a nesting scheme is used in the entanglement connection process [6,7]. Taking into account higher-order excitations, the effectively mixed entangled pair reads $\rho' = \rho + p'_2\rho'_2 + p'_3\rho'_3$, where the normalized density matrix ρ'_2 and ρ'_3 denote the two-excitation mixed state and three-excitation mixed state generated due to higher-order excitations in the spontaneous Raman process, and the small coefficients p'_2 and p'_3 are on the order of $O(\chi) \ll 1$. After the jth swapping step, the effectively entangled pair can be described as (see the Appendix, Sec. 2)

$$\rho'_{s_j} = p_{2s_j}\rho_{2s_j} + p_{1s_j}\rho_{1s_j} + p_{0s_j}\rho_{0s_j} + p'_{2s_j}\rho'_{2s_j} + p'_{3s_j}\rho'_{3s_j}. \tag{13}$$

Here ρ_{2s_j} is the maximally entangled state between two memory qubits at a distance of $L = 2^j L_0$, and ρ_{1s_j} and ρ_{0s_j} are also the maximally mixed state and vacuum state, respectively. Note that $\rho'_{s_1} = \rho'$ is just the mixed entangled state created after the first entanglement swapping step. The coefficients can be estimated to be

$$p'_{2s_j} \sim O(j\chi), p'_{3s_j} \sim O(\chi), \tag{14}$$

$$p_{\alpha s_j} \approx p_{\alpha s_{j-1}} + O(j\chi) \quad (\alpha = 0,1,2). \tag{15}$$

From Eq. (14), it is easy to see that the contributions from higher-order excitations ρ'_{2s_j} and ρ'_{3s_j} can be safely neglected, as long as the small excitation probability fulfills $j\chi \ll 1$, which can be easily achieved by tuning the write laser pulse. One can also see that the coefficients p_{2s_j}, p_{1s_j}, and p_{0s_j} are stable to the first order, therefore the probability to find an entangled pair in the remaining memory qubits is almost a constant and will not decrease significantly with distance during the entanglement connection process. The time needed for the jth connection step satisfies the iteration formula $T_{s_j} = \frac{1}{p_{s_j}}[T_{s_{j-1}} + 2^{j-1}T_{cc}]$ with p_{s_j} the success probability

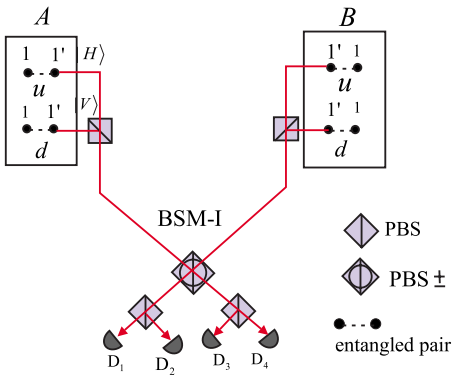

FIG. 7. (Color online) Elementary entangled pairs are first locally generated via the standard DLCZ protocol. The anti-Stokes photons are subject to BSM-i to connect neighboring communication nodes. We also assume the anti-Stokes photons retrieved from atomic ensembles at the same site have different polarization. Note that BSM-i also helps to eliminate the spurious contributions from higher order excitations.

of the jth swapping step. The total time needed for the entanglement connection process is

$$T_{tot} \approx T_0 \prod_j p_{s_j}^{-1} \approx \frac{T_{cc}}{\chi^2 \eta_1^2} e^{L_0/Latt} (L/L_0)^{\log_2^{1/\eta}}, \qquad (16)$$

where $\eta = \eta_r^2 \eta_1^2$ is a constant. The excitation probability can be estimated to be $\chi \sim L_0/L$, and then the time needed in the entanglement connection process $T_{tot} \propto (L/L_0)^{2+\log_2^{1/\eta}}$ scales polynomially or quadratically with the communication distance.

One can modify our protocol by performing entanglement generation locally and entanglement swapping remotely. It will help to increase the scalability, since entanglement generation is usually the rate-limiting stage due to the low excitation probability. Local entanglement can also be generated via the standard DLCZ protocol and then connected by two-photon Hong-Ou-Mandel interference, because local path length fluctuations can be well-controlled. The experimental setup is shown in Fig. 7. Here we need BSM-I to eliminate spurious contributions from high-order excitations. Note that the setup in Fig. 7 is a simple variation of the scheme due to Jiang *et al.* [25], where entanglement generation is performed remotely and entanglement swapping is performed locally. We remark that this simple modification is crucial to long-distance quantum communication, as entanglement generation relies on single-photon interference and must be performed locally.

C. Alternative approach

The locally entangled memory qubits can be generated by other means. Atomic ensembles can also serve as a quantum memory to store a photonic state [32,33]. By applying a time-dependent classical control laser pulse of a Rabi frequency Ω_c, the whole system has a particular zero-energy eigenstate, i.e., the dark-state-polariton. The single-polariton state is $|D,1\rangle = \frac{\Omega_c(t)}{\sqrt{\Omega_c^2(t)+g^2N}} |1\rangle_p |0\rangle_a - \frac{g\sqrt{N}}{\sqrt{\Omega_c^2(t)+g^2N}} |0\rangle_p S^\dagger |0\rangle_a$, with g

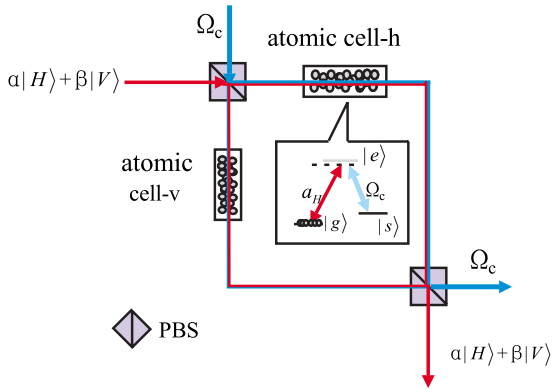

FIG. 8. (Color online) Quantum memory for photonic polarization qubits. Two ensembles are driven by a classical control field. Classical and quantized light fields are fed into the first PBS and will leave at two different outputs of the second PBS. As each atomic cell works as a quantum memory for single photons with polarization $|H\rangle$ or $|V\rangle$ via the adiabatic transfer method, the whole setup is then a quantum memory of any single-photon polarization states. The inset shows the relevant level structure of the atoms. The $|e\rangle - |s\rangle$ transition is coherently driven by the classical control field of Rabi frequency Ω_c, and the $|g\rangle - |e\rangle$ transition is coupled to a quantized light field.

being the coupling constant for the $|g\rangle - |e\rangle$ transition. Here $|0\rangle_p$ ($|1\rangle_p$) is the vacuum (single-photon) state of the quantized field to be stored. The quantum memory works by adiabatically changing $\Omega_c(t)$ such that one can coherently map $|D,1\rangle$ onto either a purely atomlike state $|0\rangle_p S^\dagger |0\rangle_a$ where the single photon is stored, or a purely photonlike state $|1\rangle_p |0\rangle_a$, which corresponds to the release of the single photon.

To exploit the advantage of two-photon Hong-Ou-Mandel-type interference, we need a quantum memory for the photonic polarization qubits. Figure 8 shows quantum memory for storing any single-photon polarization states by the dark-state-polariton method. Two atomic ensembles being a quantum memory for polarization qubits at each node are thus the required localized memory qubit in our scheme. Thus transformation between an arbitrary photon polarization state $\alpha|H\rangle + \beta|V\rangle$ and the corresponding state stored in atomic ensembles $(\alpha S_h^\dagger + \beta S_v^\dagger)|0\rangle$ can be achieved by adiabatically manipulating the control laser pulse. Importantly, our quantum memory works even when the two probability amplitudes in the stored state $\alpha|H\rangle + \beta|V\rangle$ are not c-numbers but quantum states of other photonic qubits. As a result, two memory qubits U and D at one site [see Fig. 9(a)] can be deterministically entangled in their "polarizations" by storing two polarization-entangled photons, e.g., $\frac{1}{\sqrt{2}}(S_{h_U}^\dagger S_{h_D}^\dagger + S_{v_U}^\dagger S_{v_D}^\dagger)|\text{vac}\rangle \leftrightarrow \frac{1}{\sqrt{2}}(|H\rangle|H\rangle + |V\rangle|V\rangle)$. The latter are entangled by a deterministic polarization-entangler using four single photons, linear optics, and an event-ready detection. With an overall success probability of $\frac{1}{8}$ for perfect photon counting, such an "event-ready" entangler can deterministically generate two maximally polarization-entangled qubits (see the Appendix Sec. 3).

Polarization encoding allows a two-photon interference entanglement swapping to construct entanglement between adjacent sites. As shown in Fig. 9, one can first create each

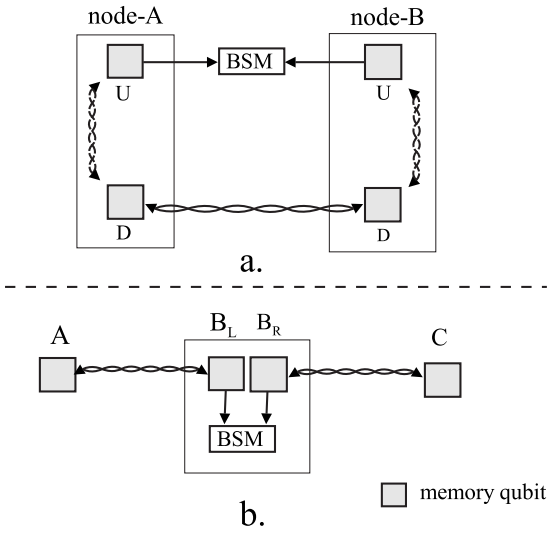

FIG. 9. (a) Entanglement swapping between adjacent communications nodes A and B. Two pairs of entangled memory qubits are first generated by storing the event-ready entanglement of two photons at each node. Then the two photons stored in the U memory at the two nodes are simultaneously retrieved and subject to a two-photon BSM at the middle point. This entanglement swapping process will in an event-ready way entangle the two distant D memory qubits. (b) Entanglement connection to extend the communication length. Two well-entangled pairs of memory qubits, one across nodes (A,B_L) and (B_R,C) are prepared in parallel. The BSM on the two photons released simultaneously from the two memories at node B results in, with a probability of 1/2, well-entangled quantum memories across nodes A and C in a definite Bell state.

memory pair in maximal event-ready entanglement at two adjacent communication nodes and then the two photons stored in the two U memories are simultaneously retrieved and subject to a two-photon BSM at the middle point. Conditioned on the result of this BSM, the remaining two D memory qubits are maximally entangled, also in an event-ready way. Usual entanglement swapping can be applied to the polarization encoding memory qubits and thus allows the implementation of a robust quantum repeater.

D. Entanglement purification

With imperfect entanglement and erroneous local operations, entanglement connection, together with decoherence, will reduce the fidelity of entanglement. Then at a certain stage of entanglement connection, the less entangled states have to be purified via the entanglement purification protocol [34,35] to enable further entanglement connection. Figure 10 shows how to achieve linear optical entanglement purification between any specified two nodes, e.g., node-I and node-J, across which one has less entangled pairs of quantum memories.

Assume two effectively mixed entangled pairs of fidelity F are created in parallel via entanglement connection as we discussed above. The effectively entangled states stored in the four memory qubits are converted into entangled photons by the read laser pulses, and then subject to two PBSs, respectively. The photons in mode b_1 and b_2 are detected in the

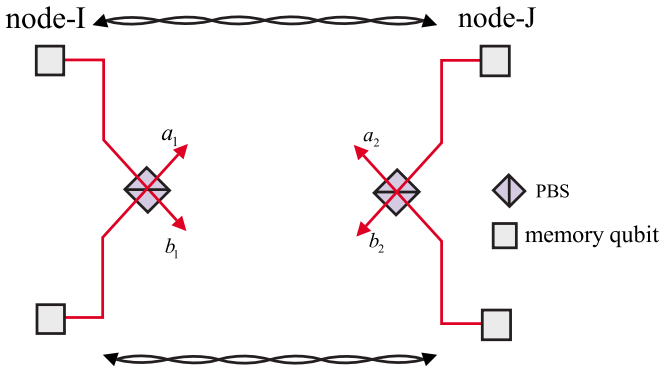

FIG. 10. (Color online) Setup for quantum entanglement purification. Entangled states have been prepared in the memory qubits between two distant nodes I and J. The memory qubits at the two sites are illuminated by a near resonant read laser pulse, and the retrieved entangled photon pairs are directed to two PBS, respectively. The photons in mode b_1 and b_2 are detected in the $|\pm\rangle = \frac{1}{\sqrt{2}}(|H\rangle \pm |V\rangle)$ basis and the remaining photons in mode a_1 and a_2 are restored in the memory qubits at the two sites, respectively.

$|\pm\rangle = \frac{1}{\sqrt{2}}(|H\rangle \pm |V\rangle)$ basis by single photon detectors, and will project the photons in mode a_1 and a_2 into an effectively maximally entangled state of higher fidelity F' (see the Appendix, Sec. 4). The higher-fidelity entangled pair in mode a_1 and a_2 can be restored into two distant memory qubits at nodes I and J by means of the dark-state-polariton method for further manipulation.

To generate a remote entangled pair, the nested quantum purification has to be implemented [6,7]. The total time overhead to create entanglement across two communication nodes at a distance of 1280 km can be numerically estimated. In our calculation, we assume the distance $L_0 = 10$ km and the photon loss rate is 0.1 dB/km in free space. To improve the scalability, we assume entanglement generation is performed locally and the entanglement generation time is considered to be 100 μs. The fidelity of the adjacent entangled memory qubits is $F=0.88$, as can be estimated by connecting two adjacent memories from two pairs of photon-memory entanglement after 5 km free space transmission of both photons [36]. One of the major factors affecting the efficiency of our scheme is single-photon detection. Fortunately, high-efficiency photon counting is feasible by using quantum state transfer and state-selective fluorescence detection with nearly unit efficiency [37,38]. To increase the efficiency, we assume photon counting detectors with detection efficiency 99% are used, and the retrieve efficiency is considered to be 98%. Entanglement purification is performed three times during the entanglement connection process to improve the fidelity. Our numerical results give a total time of about 23 s to create an effectively entangled pair, with a probability of 0.75 to get the entangled pair of fidelity 94%.

E. Comparison between different schemes

Recently, several atomic ensemble based quantum repeater schemes were proposed building on the DLCZ protocol. These schemes still have the phase stability problem since single-photon interference is also used in some stages.

The scheme presented in Ref. [25] is similar to our protocol, where they gave a detailed analysis on the superior scalability of polarization encoding. However, single-photon interference is used in the entanglement generation process, and thus entanglement generation should be performed locally. As we have discussed in Sec. III, a simple modification of their original scheme allows the implementation of a robust quantum repeater. In Ref. [39], Simon *et al.* proposed a quantum repeater, where they suggested to make entanglement generation attempts many times with the help of photon pairs and multimode memories. The use of multimode memories promises a speedup in entanglement generation by several orders of magnitude. However, entanglement generation and entanglement swapping in this protocol need single-photon interference. The remaining phase stabilization problem can be overcome by using those cases where the entaglement swapping succeeds at the same time for the upper and lower chains [40], since the phase instability should be controlled during the whole entanglement connection process, but not only in entanglement generation process. Besides, the fidelity of the final entanglement is sensitive to phase instability due to the lack of entanglement purification. It was pointed out that in this type of protocol, an initial small phase error will induce the final entanglement fidelity no more than 65% [25].

The ideas of polarization encoding, two-photon BSM, and active entanglement purification presented in our protocol are crucial to long distance quantum communication. The combination of these ideas enables a realistic fault-tolerant quantum repeater with atomic ensembles and linear optics.

IV. CONCLUSION

In summary, we have given a particular analysis on the phase stability problem of the DLCZ protocol. This problem can be overcome by taking advantage of two-photon Hong-Ou-Mandel-type interference, which alleviates the phase stability requirements by about seven orders of magnitude. Most of the ingredients in our protocol have been experimentally realized in recent years [23,29]. A long storage time is crucial for implementing atomic ensemble based quantum repeater protocol. Storage time of up to 30 μs was reported recently [13]. An optical dipole trap may have the potential to extend the storage time to 1 s. According to a recent proposal, quantum memory with nuclear atomic spins might have a very long storage time of hours [41]. Our scheme also relies on the ability to reliably transfer of photon's polarization states over a free-space or optical fiber channel. Two recent experiments demonstrated this ability up to 100 km in free space [42] and in fiber [43]. Our scheme faithfully implements a robust quantum repeater and thus enables a realistic avenue for relevant long-distance quantum communication.

ACKNOWLEDGMENTS

We are grateful to Q. Zhang and X.-M. Jin for helpful discussions. This work was supported by the National Fundamental Research Program (under Grant No. 2006CB921900), the CAS, the NNSFC, the DFG, the Alexander von Humboldt Foundation, and the Marie Curie Excellence Grant from the EU. Y.-A. Chen acknowledges additional support from the Deutsche Telekom Stiftung. Z-B.C. was also suported by the Fok Ying Tung Education Foundation.

APPENDIX: EVALUATION OF COEFFICIENTS

1. Entanglement swapping

In practice, the retrieve efficiency η_r is limited by the optical depth of the atomic ensemble and single photon detectors cannot resolve the photon number. Thus the three-photon and four-photon coincidences are also registered when performing BSM-II, which will result in an effectively entangled state $\rho=p_2\rho_2+p_1\rho_1+p_0\rho_0$. The unnormalized coefficients are calculated to be

$$p_2^{(u)}=\frac{\eta_r^2\eta_1^2}{32}, \tag{A1}$$

$$p_1^{(u)}=\frac{\eta_r^2(1-\eta_r)\eta_1^2}{16}+\frac{\eta_r^3}{32}\left(\frac{\eta_1\eta_2}{2}+\eta_1^2\right), \tag{A2}$$

$$p_0^{(u)}=\frac{\eta_r^3}{32}(1-\eta_r)\left(\frac{1}{2}\eta_1\eta_2+\eta_1^2\right)+\frac{\eta_r^2(1-\eta_r)^2\eta_1^2}{32}+\frac{\eta_r^4}{64}\left(\frac{1}{4}\eta_2^2+\eta_1^2\right), \tag{A3}$$

where η_1 and η_2 are the detector efficiency for the single photon state and two photon state. The success probability of entanglement swapping is $p=p_2^{(u)}+p_1^{(u)}+p_0^{(u)}$.

2. Entanglement connection

Considering high-order excitations in the spontaneous Raman process, the effectively entangled pair can be described by $\rho'=\rho+p_2'\rho_2'+p_3'\rho_3'$. Here we introduce a two-excitation density matrix ρ_2', containing the terms $S_{u_A}^{\dagger 2}$, $S_{d_C}^{\dagger 2}$, $S_{u_A}^{\dagger}S_{d_A}^{\dagger}$, $S_{u_A}^{\dagger}S_{u_C}^{\dagger}$ etc., and three-excitation density matrix ρ_3', containing the terms $S_{u_A}^{\dagger 2}S_{u_C}^{\dagger}$, $S_{d_C}^{\dagger 2}S_{u_A}^{\dagger}$, $S_{u_A}^{\dagger}S_{u_C}^{\dagger}S_{d_C}^{\dagger}$, $S_{u_A}^{\dagger}S_{d_A}^{\dagger}S_{u_C}^{\dagger}$, etc., to denote the contributions from higher-order excitations. The small efficient p_2' and p_3' are on the order of $O(\chi)\ll 1$. When implementing nesting entanglement connection, the effectively entangled state reads $\rho_{s_j}'=p_{2s_j}\rho_{2s_j}+p_{1s_j}\rho_{1s_j}+p_{0s_j}\rho_{0s_j}+p_{2s_j}'\rho_{2s_j}'+p_{3s_j}'\rho_{3s_j}'$. The unnormalized coefficients can be calculated to be

$$p_{2s_j}^{(u)}\approx\frac{1}{2}p_{2s_{j-1}}^2\eta, \tag{A4}$$

$$p_{1s_j}^{(u)}\approx\frac{1}{2}\eta[p_{1s_{j-1}}p_{2s_{j-1}}+O(p_{2s_{j-1}}p_{2s_{j-1}}')+O(p_{1s_{j-1}}p_{2s_{j-1}}')+O(p_{0s_{j-1}}p_{3s_{j-1}}')], \tag{A5}$$

$$p_{0s_j}^{(u)} \approx \frac{1}{8}\eta[p_{1s_{j-1}}^2 + O(p_{0s_{j-1}}p'_{2s_{j-1}})], \tag{A6}$$

$$p'^{(u)}_{2s_j} \sim O(p_{2s_{j-1}}p'^2_{2s_{j-1}}\eta) + O(p_{1s_{j-1}}p'_{3s_{j-1}}\eta), \tag{A7}$$

$$p'^{(u)}_{3s_j} \sim O(p_{2s_{j-1}}p'_{3s_{j-1}}\eta), \tag{A8}$$

with $\eta=\eta_1^2\eta_r^2$, where the three-photon coincidence counts are safely neglected. From the above equations, we find that

$$\frac{p'^{(u)}_{3s_j}}{p^{(u)}_{2s_j}} \sim O\left(\frac{p'_{3s_{j-1}}}{p_{2s_{j-1}}}\right) \sim O\left(\frac{\chi}{p_2}\right), \tag{A9}$$

$$\frac{p'^{(u)}_{2s_j}}{p^{(u)}_{2s_j}} \sim O\left(\frac{p'_{2s_{j-1}}}{p_{2s_{j-1}}}\right) + O\left(\frac{p'_{3s_{j-1}}}{p_{2s_{j-1}}}\right) \sim O\left(\frac{j\chi}{p_2}\right), \tag{A10}$$

$$\frac{p^{(u)}_{1s_j}}{p^{(u)}_{2s_j}} \approx \frac{p_{1s_{j-1}}}{p_{2s_{j-1}}} + O\left(\frac{p'_{3s_{j-1}}}{p_{2s_{j-1}}}\right) + O\left(\frac{p'_{2s_{j-1}}}{p_{2s_{j-1}}}\right), \tag{A11}$$

$$\frac{p^{(u)}_{0s_j}}{p^{(u)}_{2s_j}} \approx \frac{1}{4}\left(\frac{p_{1s_{j-1}}}{p_{2s_{j-1}}}\right)^2 + O\left(\frac{p'_{2s_{j-1}}}{p_{2s_{j-1}}}\right), \tag{A12}$$

where we have considered that the coefficients $p_{2s_{j-1}}$, $p_{1s_{j-1}}$, and $p_{0s_{j-1}}$ are on the same order of magnitude. Finally, we conclude that during the nesting entanglement connection process, the coefficients can be estimated to be

$$p'_{3s_j} \sim O(\chi), p'_{2s_j} \sim O(j\chi), \tag{A13}$$

$$p_{\alpha s_j} \approx p_{\alpha s_{j-1}} + O(j\chi). \tag{A14}$$

The success probability of the jth entanglement connection is $p_{s_j}=p^{(u)}_{2s_j}+p^{(u)}_{1s_j}+p^{(u)}_{0s_j}$.

3. Deterministic entangler

The deterministic single-photon polarization entangler is depicted in Fig. 11. The input state is $|-\rangle_1|V\rangle_2|+\rangle_{1'}|H\rangle_{2'}$. In the ideal case where single photons can be created on demand and photon-number counting detectors are used to identify the Bell states, we will obtain two maximally entangled photons in $|\psi^+\rangle_{ab}$ or $|\phi^-\rangle_{ab}$, conditioned on a coincidence count in two of the four detectors with a success probability $\frac{1}{8}$ [44].

However, current single photon sources are probabilistic and the most used single photon detectors cannot distinguish between one and more than one detected photons. Due to these imperfections, the output state in a and b is not a pure state but a mixed entangled state. Assuming the single photon sources can generate single photons with probability p_r, it is easy to see that when there are two photons $(\{1,2\},\{1,2'\},\{1',2\},\{1',2'\})$ with probability $p_r^2(1-p_r)^2$, three photons $(\{1,1',2\},\{1,1',2'\},\{1,2,2'\},\{1',2,2'\})$ with probability $p_r^3(1-p_r)$, and four photons $(\{1,1',2',2'\})$

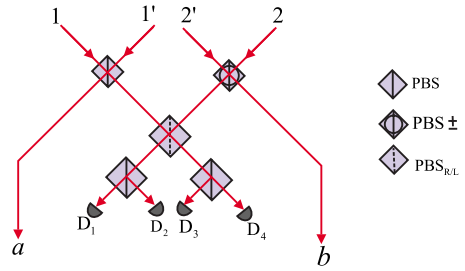

FIG. 11. (Color online) Deterministic single-photon polarization entangler. PBS (PBS$_\pm$; PBS$_{R/L}$) reflects photons with vertical polarization $|V\rangle(|-\rangle);|L\rangle$ and transmits photons with horizontal-polarization $|H\rangle$ $(|+\rangle;|R\rangle)$. Here $|\pm\rangle=\frac{1}{\sqrt{2}}(|H\rangle+|V\rangle);|R/L\rangle=\frac{1}{\sqrt{2}}(|H\rangle\pm i|V\rangle)$. The four single photons are prepared on demand in an initial state $|-\rangle_1|V\rangle_2|+\rangle_{1'}|H\rangle_{2'}$. After passing through the first PBS and PBS$_\pm$, one selects the "four-mode" case where there is one and only one photon in each of the four output modes. Then the BSM will collapse photons in modes a and b into a Bell state conditioned on the result of the BSM. In our case, a coincidence count between single-photon detectors D1 and D4 (D1 and D3) or between D2 and D3 (D2 and D4) leaving photons along paths a and b deterministically entangled in $|\psi^+\rangle_{ab}(|\phi^-\rangle_{ab})$.

with probability p_r^4 emitted from single photon sources, there will be a coincidence count between two of the detectors.

Considering all these possibilities, we find that if one of the four coincidence counts occurs, e.g., D_1 and D_4 is registered, the output state in a and b is equivalent to an effectively maximally entangled state

$$\rho_c = p_{2c}\rho_{2c} + p_{1c}\rho_{1c} + p_{0c}\rho_{0c}, \tag{A15}$$

with the unnormalized coefficients

$$p^{(u)}_{2c} = \frac{p_r^4\eta_1^2}{32}, \tag{A16}$$

$$p^{(u)}_{1c} = \frac{p_r^3(1-p_r)\eta_1^2}{8} + \frac{p_r^4\eta_1^2}{32} + \frac{p_r^4\eta_1\eta_2}{64}, \tag{A17}$$

$$p^{(u)}_{0c} = \frac{1}{32}[p_r^3(1-p_r)(2\eta_1^2+\eta_1\eta_2) + p_r^4\eta_1\eta_2 + 4p_r^2(1-p_r^2)\eta_1^2]. \tag{A18}$$

Here ρ_{2c} is one of the maximally entangled Bell states, ρ_{1c} is the one-photon maximally mixed state, and ρ_{0c} is the vacuum state, which indicates that all the input photons are detected and there is no photon in the output a and b. After the event-ready mixed entangled state is successfully generated, it will be directed and stored into memory qubits at each communication node as discussed in the main text. The success probability for the event-ready entangler is $p_c=p^{(u)}_{2c}+p^{(u)}_{1c}+p^{(u)}_{0c}$.

4. Entanglement purification

Suppose we have generated an effectively mixed entangled state $\rho_m=p_{2m}\rho_{2m}+p_{1m}\rho_{1m}+p_{0m}\rho_{0m}$ of fidelity F

across nodes I and J. For simplicity, we assume the mixed state is of the form $\rho_{2m}=F|\phi^+\rangle_{IJ}\langle\phi^+|+(1-F)|\psi^+\rangle_{IJ}\langle\psi^+|$, with $|\phi^+\rangle_{IJ}=(S_{u_I}^\dagger S_{u_J}^\dagger+S_{d_I}^\dagger S_{d_J}^\dagger)/\sqrt{2}|\text{vac}\rangle$ and $|\psi^+\rangle_{ij}=(S_{u_I}^\dagger S_{d_J}^\dagger+S_{d_I}^\dagger S_{u_J}^\dagger)/\sqrt{2}|\text{vac}\rangle$. Two pairs of entangled memory qubits are generated in parallel. Linear optical entanglement purification will project the photons in modes a_1 and a_2 into a mixed entangled state of higher fidelity $F'=\frac{F^2}{F^2+(1-F)^2}$, which can be described as

$$\rho_p = p_{2p}\rho_{2p} + p_{1p}\rho_{1p} + p_{0p}\rho_{0p}, \tag{A19}$$

with $\rho_{2p}=F'|\phi^+\rangle_{IJ}\langle\phi^+|+(1-F')|\psi^+\rangle_{IJ}\langle\psi^+|$. The unnormalized coefficients are

$$p_{2p}^{(u)} = \frac{1}{2}p_{2m}^2\eta_r^4\eta_1^2[F^2+(1-F)^2], \tag{A20}$$

$$p_{1p}^{(u)} = p_{2m}^2\eta_r^3(1-\eta_r)\eta_1^2 + \frac{1}{2}p_{1m}p_{2m}\eta_r^3\eta_1^2 + p_{2m}^2\eta_r^4F(1-F)\eta_1\eta_2, \tag{A21}$$

$$p_{0p}^{(u)} = p_{2m}^2\left[\frac{1}{4}\eta_r^4F^2\eta_2^2 + \eta_r^3(1-\eta_r)F(1-F)\eta_1\eta_2 + \eta_r^2(1-\eta_r)^2(F+1/2)\eta_1^2 + \eta_r^3(1-\eta_r)F^2\eta_1\eta_2\right] + p_{2m}p_{1m}\left[\eta_r^2(1-\eta_r)(F_m+1/2)\eta_1^2 + \eta_r^3\frac{F}{2}\eta_1\eta_2\right] + \frac{1}{8}p_{1m}^2\eta_r^2\eta_1^2 + p_{2m}p_{0m}\eta_r^2F\eta_1^2. \tag{A22}$$

The success probability of entanglement purification is $p_p=p_{2p}^{(u)}+p_{1p}^{(u)}+p_{0p}^{(u)}$.

[1] N. Gisin *et al.*, Rev. Mod. Phys. **74**, 145 (2002).
[2] A. K. Ekert, Phys. Rev. Lett. **67**, 661 (1991).
[3] M. Zukowski, A. Zeilinger, M. A. Horne, and A. K. Ekert, Phys. Rev. Lett. **71**, 4287 (1993).
[4] J.-W. Pan, D. Bouwmeester, H. Weinfurter and A. Zeilinger, Phys. Rev. Lett. **80**, 3891 (1998).
[5] C. H. Bennett, G. Brassard, S. Popescu, B. Schumacher, J. A. Smolin, and W. K. Wooters, Phys. Rev. Lett. **76**, 722 (1996).
[6] H.-J. Briegel, W. Dür, J. I. Cirac, and P. Zoller, Phys. Rev. Lett. **81**, 5932 (1998).
[7] W. Dür, H. J. Briegel, J. I. Cirac, and P. Zoller, Phys. Rev. A **59**, 169 (1999).
[8] S. J. van Enk, J. I. Cirac, and P. Zoller, Science **279**, 205 (1998).
[9] L.-M. Duan, M. Lukin, J. I. Cirac, and P. Zoller, Nature (London) **414**, 413 (2001).
[10] A. Kuzmich *et al.*, Nature (London) **423**, 731 (2003).
[11] C. H. van del Wal *et al.*, Science **301**, 196 (2003).
[12] M. D. Eisaman *et al.*, Nature (London) **438**, 837 (2005).
[13] D. N. Matsukevich, T. Chaneliere, S. D. Jenkins, S. Y. Lan, T. A. B. Kennedy, and A. Kuzmich, Phys. Rev. Lett. **97**, 013601 (2006).
[14] S. Chen, Y. A. Chen, T. Strassel, Z. S. Yuan, B. Zhao, J. Schmiedmayer, and J. W. Pan, Phys. Rev. Lett. **97**, 173004 (2006).
[15] C. W. Chou *et al.*, Nature (London) **438**, 828 (2005).
[16] D. N. Matsukevich and A. Kuzmich, Science **306**, 663 (2004).
[17] C. W. Chou *et al.*, Science **316**, 1316 (2007).
[18] K. W. Holman, D. D. Hudson, and J. Ye, Opt. Lett. **30**, 1225 (2005).
[19] B. Zhao, Z.-B. Chen, Y.-A. Chen, J. Schmiedmayer, and J.-W. Pan, Phys. Rev. Lett. **98**, 240502 (2007).
[20] C. K. Hong, Z. Y. Ou, and L. Mandel, Phys. Rev. Lett. **59**, 2044 (1987).
[21] D. Felinto *et al.*, Nat. Phys. **2**, 844 (2006).
[22] T. Chanelière, D. N. Matsukevich, S. D. Jenkins, S. Y. Lan, R. Zhao, T. A. B. Kennedy, and A. Kuzmich, Phys. Rev. Lett. **98**, 113602 (2007).
[23] Z.-S. Yuan, Y. A. Chen, S. Chen, B. Zhao, M. Koch, T. Strassel, Y. Zhao, G. J. Zhu, J. Schmiedmayer, and J. W. Pan, Phys. Rev. Lett. **98**, 180503 (2007).
[24] A. André, Ph.D. thesis, Harvard University, 2005 (unpublished).
[25] L. Jiang, J. M. Taylor, and M. D. Lukin, Phys. Rev. A **76**, 012301 (2007).
[26] C. Simon and W. T. M. Irvine, Phys. Rev. Lett. **91**, 110405 (2003).
[27] S. Bose, P. L. Knight, M. B. Plenio, and V. Vedial, Phys. Rev. Lett. **83**, 5158 (1999); X.-L. Feng, Z. M. Zhang, X. D. Li, S. Q. Gong, and Z. Z. Xu, *ibid.* **90**, 217902 (2003); D. E. Browne, M. B. Plenio, and S. F. Huelga, *ibid.* **91**, 067901 (2003).
[28] D. E. Browne and T. Rudolph, Phys. Rev. Lett. **95**, 010501 (2005).
[29] Y.-A. Chen *et al.*, e-print arXiv:quant-ph/0705.1256v1.
[30] Note that in Ref. [19], both entanglement swapping and entanglement generation is performed remotely, so we need at least two atomic ensembles at each node. Here entanglement swapping is performed locally following the standard quantum repeater protocol [6], and thus we have to manipulate at least four atomic ensembles at each communication site.
[31] A. V. Gorshkov, A. Andre, M. Fleischhauer, A. S. Sorensen, and M. D. Lukin, Phys. Rev. Lett. **98**, 123601 (2007).
[32] M. D. Lukin, S. F. Yelin, and M. Fleischhauer, Phys. Rev. Lett. **84**, 4232 (2000).
[33] M. Fleischhauer and M. D. Lukin, Phys. Rev. Lett. **84**, 5094 (2000).
[34] J.-W. Pan *et al.*, Nature (London) **410**, 1067 (2001).
[35] J.-W. Pan *et al.*, Nature (London) **423**, 417 (2003).
[36] C.-Z. Peng *et al.*, Phys. Rev. Lett. **94**, 150501 (2005).
[37] D. F. V. James and P. G. Kwiat, Phys. Rev. Lett. **89**, 183601 (2002).
[38] A. Imamo$\bar{\text{g}}$lu, Phys. Rev. Lett. **89**, 163602 (2002).

[39] C. Simon, H. de Riedmatten, M. Afzelius, N. Sangouard, H. Zbinden, and N. Gisin, Phys. Rev. Lett. **98**, 190503 (2007).
[40] C. Simon (private communication).
[41] A. Dantan, G. Reinaudi, A. Sinatra, F. Laloe, E. Giacobino, and M. Pinard, Phys. Rev. Lett. **95**, 123002 (2005).
[42] T. Schmitt-Manderbach *et al.*, Phys. Rev. Lett. **98**, 010504 (2007).
[43] C. Z. Peng, J. Zhang, D. Yang, W. B. Gao, H. X. Ma, H. Yin, H. P. Zeng, T. Yang, X. B. Wang, and J. W. Pan, Phys. Rev. Lett. **98**, 010505 (2007).
[44] Q. Zhang *et al.*, e-print arXiv:quant-ph/0610145.